Ag(111) Surface Reconstruction Studied by Optical Second-Harmonic Generation

Yeke Tang, L. J. Simpson, and T. E. Furtak
Department of Physics, Colorado School of Mines, Golden, Colorado 80401

(Received 13 May 1991)

We have studied the optical second-harmonic reflectance of Ag(111) as a function of the incident photon energy and the interfacial potential in an electrochemical environment. The behavior of the anisotropic contribution is consistent with a potential-induced surface reconstruction from C_{3v} to C_3 under conditions of positive surface charge.

PACS numbers: 68.35.Rh, 42.65.Ky, 82.45.+z

The (111) surfaces of fcc metals are particularly stable with regard to reconstruction. Only one example (Au) has been clearly identified where this trend is broken [1,2]. The (111) surface of Ag, in particular, is stable in UHV—that is, the terminated crystal maintains the same atomic arrangement as atoms in the bulk. In general, reconstruction has been understood through a consideration of the relief of surface stress balanced by a lattice-misfit energy. In the electrochemical environment there is a large gradient in the interfacial potential difference associated with mutual screening by electrons in the metal and by ions in the solution. This leads to conditions which modify the subtle energy balance established at a free surface. Under these circumstances it may be possible to create or lift a reconstruction through external modification of the potential. This phenomenon has already been demonstrated on Au [3].

We have discovered a previously unknown surface reconstruction of Ag(111) under conditions where the metal is positively charged. The reconstruction was identified with optical second-harmonic (SH) generation spectroscopy, which is particularly sensitive to changes in the surface symmetry.

The rod-shaped Ag single crystal was mounted in Teflon with only the (111) face, 1.1 cm in diameter, exposed. This functioned as the working electrode of a standard three-electrode electrochemical cell. The cell was filled with 0.1-M K_2SO_4 (triple-distilled water, reagent-grade electrolyte, zero-grade nitrogen purging). The Ag(111) surface was mechanically polished in three steps with 1.0, 0.3, and 0.05 μm alumina, and then chemically polished using a cyanide procedure [4]. The applied potential V was scanned between -1 and 0 V at a rate of 10 mV/sec. [V is reported as the potential of the sample minus the potential of the saturated calomel electrode (SCE). This establishes a reproducible reference with an arbitrary zero. The least perturbed condition is at the potential of zero charge (PZC). For silver in contact with aqueous 0.1-M K_2SO_4, $V_{\mathrm{PZC}} \approx -0.75$ V [5].] The p-polarized light (at a fixed incident angle of 45°) came from a pulsed dye laser pumped by a 10-Hz, 20-nsec pulsewidth, frequency-doubled yttrium-aluminum-garnet laser. The incident laser beam had a size of about 0.5 cm^2 and was kept at a pulse energy below 5 mJ at the sample surface. With the use of optical filters only p-polarized SH reflections $I^{(2)}$ were collected by a monochromator and conventional gated integrating electronics.

It has been shown previously that the SH response from the unreconstructed (111) surface of fcc materials obeys C_{3v} symmetry [6]. This is due to the combination of the top two layers of the sample in influencing the second-order surface susceptibility. The form which the observed intensity follows for p polarization of both the incident light (with photon energy $\hbar\omega$) and the SH light (with photon energy $\hbar\Omega = 2\hbar\omega$) is [7]

$$I^{(2)}(\phi,\Omega,V) = \big| |a| + |c| e^{i\theta} \cos(3\phi) \big|^2 . \quad (1)$$

Here ϕ is the angle between the x axis and the projection of the incident wave vector on the surface plane (we define $\hat{z} = [111]$, $\hat{x} = [2\bar{1}\bar{1}]$, $\hat{y} = [01\bar{1}]$). For simplicity, the nonlinear dependence upon the incident intensity has been absorbed into both a and c. These coefficients also contain the nonlinear susceptibilities of the system as well as the linear optical properties of the bulk media. In our experiment the perturbation is applied parallel to the sample normal. As V changes, a, c, and θ are, in general, expected to change; however, for C_{3v} symmetry, Eq. (1) is always valid [6].

We rotated the Ag(111) crystal about its surface normal to generate the ϕ-dependent intensity consistent with Eq. (1). As an example, Fig. 1 demonstrates this anisotropic SH effect. However, it can be seen immediately that the SH intensity (a full 360° rotation) changes from a six-peak pattern (six maxima and six minima) at $V = -1$ V (a somewhat negatively charged surface) to a three-peak pattern (three maxima and three minima) at $V = 0$ V (substantial positive charge on the surface). Changes of this type have been observed in the past from Ag(111) [8,9]. However, those were based upon experiments performed at $\hbar\omega = 1.17$ eV and showed the opposite behavior with respect to the direction of the change in V (six maxima for more positive V, three maxima at more negative V). This effect subsequently associated with the presence of contamination in the sample chamber [6].

It is clear from Eq. (1) that the three parameters $|a|$, $|c|$, and θ can be extracted from $I^{(2)}$ measured at $\phi = 0°$, 30°, and 60°. For each photon energy in the range from

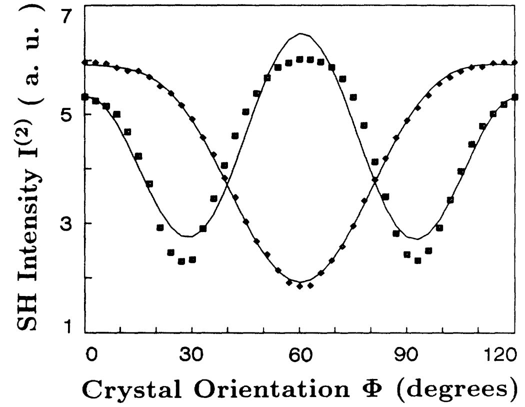

FIG. 1. Angle-dependent SH intensities at $\hbar\omega=1.94$ eV; squares at $V=-1$ V and diamonds at $V=0$ V. Both are taken for a full 360° rotation, and then averaged into one cycle of 120° to increase the signal-to-noise ratio and deemphasize any systematic errors. The solid lines are nonlinear least-squares fits to the data using Eq. (2) with $\theta_1=90°$ [from data inspection, $I^{(2)}(30°)\equiv I^{(2)}(90°)$]. The fitted parameters are, for squares, $|a|=1.6$, $|b|=0.06$, $|c|=1.8$, and $\theta_2=84.3°$, and, for diamonds, $|a|=1.9$, $|b|=1.1$, $|c|=0.5$, and $\theta_2=2.4°$.

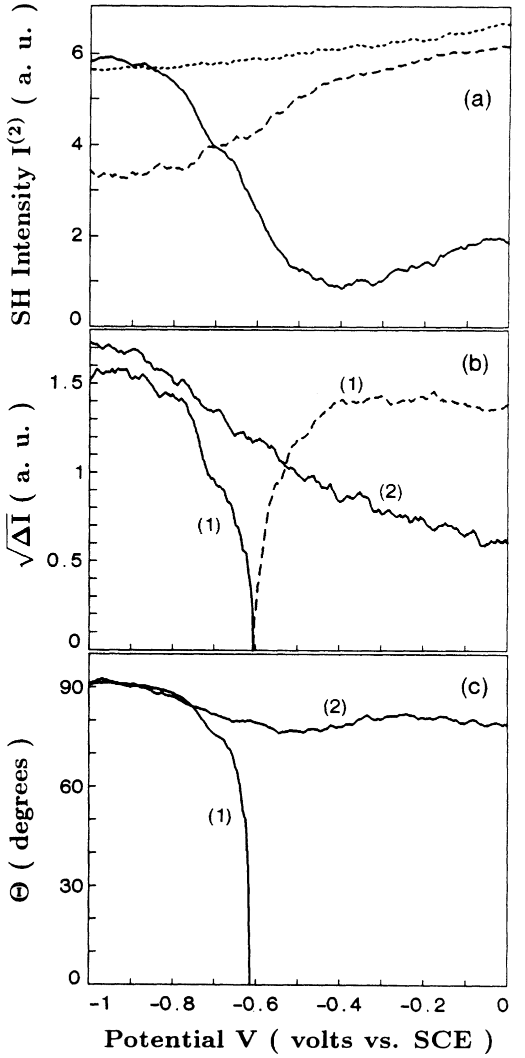

FIG. 2. (a) The SH intensities vs the interfacial potential V measured at $\hbar\omega=1.94$ eV. The solid line is $I^{(2)}(60°)$, the short-dashed line $I^{(2)}(0°)$, and the long-dashed line $I^{(2)}(30°)$. (b) The anisotropic SH response $\sqrt{\Delta I}$; curve (2) at $\hbar\omega=1.77$ eV and curve (1) at $\hbar\omega=1.94$ eV. (The dashed line corresponds to $\Delta I<0$ and is plotted as $\sqrt{|\Delta I|}$.) (c) The phase difference θ defined in Eq. (1); curve (2) at $\hbar\omega=1.77$ eV and curve (1) at $\hbar\omega=1.94$ eV.

$\hbar\omega=1.43$ eV (870 nm) to $\hbar\omega=2.25$ eV (550 nm) we recorded the V dependence of $I^{(2)}$ at these select values of ϕ. We are particularly interested in $|c|$, which contains the anisotropic second-order surface susceptibilities. This should contain the majority of the surface symmetry information. Details concerning $|a|$ are reported upon elsewhere [10].

Figure 2(a) shows a representative data set of the SH intensities obtained for $\hbar\omega=1.94$ eV (640 nm) at $\phi=0°$, 30°, and 60°, respectively. From these intensities the calculated $|c|$ and θ are plotted in Figs. 2(b) and 2(c). According to Eq. (1),

$$|c|=\{\tfrac{1}{2}[I^{(2)}(0°)+I^{(2)}(60°)]-I^{(2)}(30°)\}^{1/2}.$$

We define

$$\bar{I}^{(2)}(0°,60°)\equiv\tfrac{1}{2}[I^{(2)}(0°)+I^{(2)}(60°)],$$

the average of the intensities at 0° and 60°, and

$$\Delta I\equiv\bar{I}^{(2)}(0°,60°)-I^{(2)}(30°).$$

Thus, when Eq. (1) applies, ΔI measures $|c|^2$. Normally, Eq. (1) is adequate in explaining both six-peak and three-peak patterns as long as ΔI is positive. As ΔI decreases the SH intensity evolves from a six-peak pattern to three-peak pattern (see Fig. 1). We have observed this six-peak to three-peak pattern evolution in the whole spectral range of our study. A correlated slow and monotonic decrease in $\sqrt{\Delta I}$ is also evident for most of the spectral range [as is seen in curve (2) in Fig. 2(b) for $\hbar\omega=1.77$ eV].

Dramatically different behavior is associated with a narrow range of $\hbar\omega$ between about 1.85 eV (670 nm) and 1.97 eV (630 nm). Within this narrow spectral range we see an abrupt drop in ΔI vs V. For more positive V, ΔI crosses zero and becomes negative, which Eq. (1) forbids. Figure 2(b) shows $\sqrt{|\Delta I|}$, which emphasizes the change. The change between the normal region and this anomalous region, as well as the interpretation of the origin of this anomalous behavior, is the main point of this paper.

Because the threefold rotational symmetry is obviously maintained for both three-peak and six-peak SH intensity patterns, the simplest correction to Eq. (1) to account for a negative ΔI would be an additional term proportional to $\sin(3\phi)$. Then the SH intensity would have the form

$$I^{(2)}(\phi)=\left|\,|a|+|b|e^{i\theta_1}\sin(3\phi)+|c|e^{i\theta_2}\cos(3\phi)\right|^2 . \tag{2}$$

With Eq. (2), ΔI is $|c|^2-|b|^2$ and could become negative if $|b|$ is sufficiently large. Equation (2) is consistent with a system displaying C_3 symmetry or with a system maintaining C_{3v} symmetry whose mirror planes have been rotated. However, the latter would show a potential-dependent shift of the entire pattern with respect to the $\phi=0$ condition. This was not observed. We therefore associate the anomalous region with a reconstruction under which the surface changes from C_{3v} symmetry to C_3 symmetry. The six-peak to three-peak pattern change itself does not necessarily indicate a reconstruction, but a reconstruction is the most appropriate explanation when $\Delta I<0$. The reconstruction is observed as the potential is changed from -1 V (a six-peak pattern consistent with C_{3v} symmetry and $\Delta I>0$) to 0 V (a three-peak pattern consistent with C_3 symmetry and $\Delta I<0$).

Potential-induced reconstructions have already been identified by SH reflectance and by x-ray techniques on Au(111) and Au(100) [3,11]. However, those systems also display reconstruction in UHV (where the structure is a function of temperature). Prior to our work, the Ag(111) surface was thought to be structurally stable for all conditions except for one case involving strongly chemisorbed material (Ag-I) [12].

To more clearly identify the transition we establish V_0 as the potential where ΔI becomes zero. V_0 is plotted versus the SH energy, $\hbar\Omega$, in Fig. 3. The solid line is a parabolic fit to the data points (squares), and it is intended to provide a qualitative separation between the regions of $\Delta I<0$ (inside the parabolic curve) and $\Delta I>0$ (outside). Note that the entire parabolic curve is found at potentials positive of the zero charge condition. This means $\Delta I<0$ occurs when the Ag surface becomes electron deficient, when surface electron energy levels become more positive than those in the bulk, and when negatively charged ions are more likely to populate the solution side of the interface. Any of these effects could potentially lead to surface reconstruction.

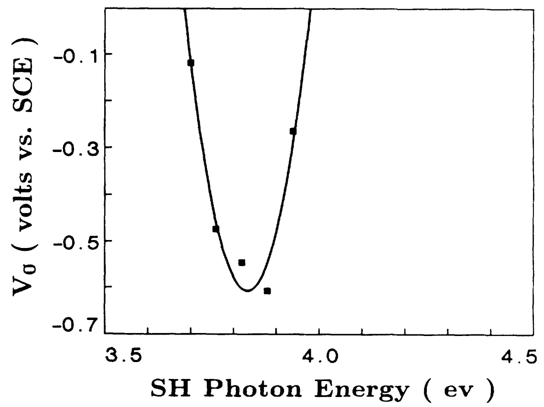

FIG. 3. Squares, from right to left, for $\hbar\omega$ at 1.97, 1.94, 1.91, 1.88, and 1.85 eV, respectively, represent the potential V_0 where ΔI crosses zero. The solid line is an aid to the visual separation of regions where $\Delta I<0$ from those where $\Delta I>0$.

From Fig. 3 it is clear that V_0 depends upon $\hbar\Omega$. A structural phase transition should occur at a single well-defined potential. However, in SH spectroscopy our ability to detect a given susceptibility component depends upon its relative magnitude. A resonance in terms contained within $|b|$, such as χ_{yyy}, would explain the $\hbar\Omega$ dependence of V_0. It is significant to note that $\hbar\Omega=3.88$ eV, where the transition is most apparent, is close to the interband transition energy in Ag. This could mean that a potential-dependent surface state is involved [13]. The latter, which might appear on the C_3 surface, would display a V-dependent energy, and would be associated with resonance confined to a narrow range of $\hbar\Omega$.

Since the abrupt potential-dependent change of $\sqrt{\Delta I}$ near V_0 is associated with a possible surface structural phase transition, it is natural to examine how $\sqrt{\Delta I}$ approaches zero from $\Delta I>0$ [where Eq. (1) is still meaningful] using a power-law function [14]:

$$\sqrt{\Delta I}=A|v|^{\beta} . \tag{3}$$

$\sqrt{\Delta I}=(|c|^2-|b|^2)^{1/2}$ measures the relative change between $|c|$ and $|b|$, which are related to χ_{xxx} and χ_{yyy}, respectively. The size of $\sqrt{\Delta I}>0$ measures the extent of the surface involved with C_{3v} symmetry. Therefore it can be treated as an order parameter as the transition is approached from the negative potential side. The reduced potential

$$v=\frac{V-V_0}{V_0-V_{\mathrm{PZC}}}$$

is related to the electrochemical contribution to the free energy of the system. A log-log plot of $\sqrt{\Delta I}$ vs $|v|$ displays a particularly good straight-line behavior at $\hbar\Omega=3.88$ eV (see the squares in Fig. 4). A linear least-squares fit to the data yields $\beta=0.39$. This kind of power-law function is characteristic of an order parameter near a second-order phase transition. In its more common embodiment, temperature is the thermodynamic variable and the critical exponent β is measured to be somewhere close to $\frac{1}{3}$ [14].

The transition can also be observed in a plot of θ vs V [Fig. 2(c)]. Within the limited spectral range, θ switches abruptly from $\sim 90°$ to 0° near V_0. Away from this transition (where $\Delta I \gg 0$), θ is close to 90° and shows very little dependence on potential. When $\Delta I<0$ the isotropic (a) and the anisotropic (c) contributions to the SH intensity are in phase with each other.

One mechanism which explains the nature of the transformation involves the generation of buckling in the top Ag layer. This could be accommodated by a slight dis-

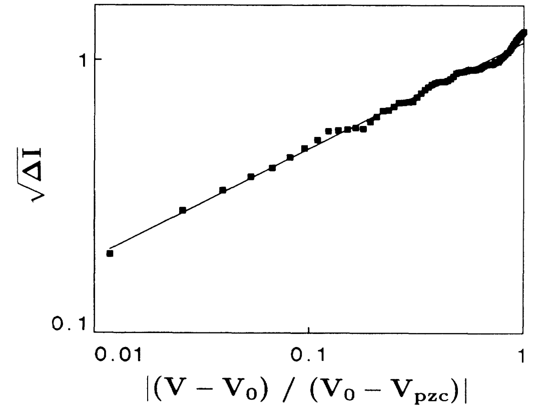

FIG. 4. Log-log plot of $\sqrt{\Delta I}$ vs the reduced potential for $\hbar\omega = 1.94$ eV from $V = V_{PZC}$ to $V = V_0$ where $\Delta I > 0$. The solid line is a linear least-squares fit using Eq. (3) and the slope or the power-law exponent $\beta = 0.39$.

placement along z leading to a $(\sqrt{3}\times\sqrt{3})R30°$ surface. Provided each of the three atoms in the surface unit cell were electronically distinct, together with the underlying undisturbed Ag layer, the resulting surface susceptibility would obey C_3 symmetry. All mirror planes are lost in this transformation. The resulting structure would show an altered electron density versus z. This could be verified in a grazing incidence *in situ* x-ray reflectance experiment.

We have shown that the crystallographic dependence of optical SH generation from a Ag(111) electrode has suggested the existence of a previously unexpected potential-induced surface reconstruction from C_{3v} to C_3 symmetry. The characteristics of this effect obey a phenomelogical power law with a critical exponent close to 0.39 at $\hbar\Omega \approx 3.88$ eV. This behavior is detected only because of a possible resonance in the χ_{yyy} surface susceptiblity which may be related to a surface state connected with the reconstructed condition.

This work was supported by the U.S. Department of Energy under Grant No. DE-FG02-86ER45253. We thank B. M. Ocko for some productive discussions.

[1] Š. Pick, Surf. Sci. Rep. **12**, 99 (1991).

[2] A. R. Sandy, S. G. J. Mochrie, D. M. Zehner, K. G. Huang, and Doon Gibbs, Phys. Rev. B **43**, 4667 (1991).

[3] A. Fredrich, B. Pettinger, D. M. Kolb, G. Lüpke, R. Steinhoff, and G. Marowsky, Chem. Phys. Lett. **163**, 123 (1989).

[4] A. Bewick and B. Thomas, J. Electroanal. Chem. **65**, 911 (1975).

[5] G. Valette and A. Hamelin, C. R. Acad. Sci. **279**, 295 (1974).

[6] G. L. Richmond, J. M. Robinson, and V. L. Shannon, Prog. Surf. Sci. **28**, 1 (1988).

[7] J. E. Sipe, D. J. Moss, and H. M. van Driel, Phys. Rev. B **35**, 1129 (1987).

[8] V. L. Shannon, D. A. Koos, and G. L. Richmond, J. Phys. Chem. **91**, 5548 (1987).

[9] O. A. Aktsipetrov, A. M. Brodskii, L. I. Daikhin, A. V. Ermushev, T. V. Murzina, A. V. Petukhov, S. K. Sigalaev, and A. M. Funtikov, Pis'ma Zh. Tekh. Fiz. **59**, 86 (1989) [Sov. Tech. Phys. Lett. **34**, 550 (1989)]; Électrokhimiya **25**, 1573 (1989).

[10] T. E. Furtak, Yeke Tang, and L. J. Simpson (to be published).

[11] B. M. Ocko, J. Wang, A. Davenport, and H. Isaacs, Phys. Rev. Lett. **65**, 1466 (1990).

[12] Ghaleb N. Salaita, Frank Lu, Laarni Laguren-Davidson, and Arthur T. Hubbard, J. Electroanal. Chem. **229**, 1 (1987).

[13] D. M. Kolb and C. Franke, Appl. Phys. A **49**, 379 (1989).

[14] H. E. Stanley, *Introduction to Phase Transition and Critical Phenomena* (Clarendon, Oxford, 1971).